A spin density wave in the topological insulator Bi_2Te_3

Anjan Soumyanarayanan*
Massachusetts Institute of Technology

May 11, 2010

Abstract

Topological insulators are materials with a bulk band gap, but with topologically protected, spin polarized surface states with Dirac dispersion. Bi_2Te_3 is such a topological insulator with a single Dirac cone at the center of the Brillouin zone. ARPES studies have shown that the Fermi surface of Bi_2Te_3 changes from a circle to a hexagon, and then to a hexagram, when moving away from the Dirac point. This has been explained in literature by the addition of a warping term added to the Dirac Hamiltonian, which leads to more exotic spin texture. This manuscript elaborates on hexagonal warping in Bi_2Te_3, and examines a possible spin density wave (SDW) state due to warping. Using Landau–Ginzburg formalism, we find that a correspondence between the SDW state and the cubic anisotropy problem. Using this, we construct a phase diagram of spin order in on the hexagonal Fermi surface of Bi_2Te_3.

CONTENTS

I. Topological Band Insulators 1
A. The Quantum Hall Insulator . . . 1
B. The Quantum Spin Hall Effect . . . 1
C. 3D Topological Insulators . . . 2

II. A Warped Helical Fermi Surface 2
A. Fermi Surface Warping in Bi_2Te_3 . . . 2

III. SDW State in a Warped Dirac Cone 3
A. Spin Density Waves . . . 3
B. Fermi Surface Nesting in Bi_2Te_3 . . . 4
C. Landau–Ginzburg Theory of SDW State . . . 4
D. Cubic Anisotropy in SDW State . . . 5

IV. Conclusions 5

References 6

I. TOPOLOGICAL BAND INSULATORS

The concept of broken symmetry has been central to condensed matter physics. Systems of interest can be characterized by the symmetries that are spontaneously broken at a phase transition, *e.g.* translational symmetry for a crystalline solid and rotational symmetry for a magnet. Superfluids and superconductors that break a more subtle gauge symmetry have been intensely studied over the past century. All these systems can be described by the Landau–Ginzburg framework of phase transitions, where an order parameter emerges below a critical temperature T_c [1–3]. Landau–Ginzburg theory, used in conjunction the renormalization group (RG) technique[2], has been extremely successful in describing critical phenomena and phase transitions with spontaneous broken symmetries.

A. The Quantum Hall Insulator

The quantum Hall state, discovered in 1980, was the first known macroscopic quantum state with no spontaneously broken symmetry[4]. The notion of order in the quantum Hall state is topological in nature, and is insensitive to small perturbations (*e.g.* weak disorder) and smooth changes in tuning parameters (*e.g.* material composition), unless the system passes through a quantum phase transition[4;5].

Ordinary insulators are characterized by a Fermi energy located in the bulk band gap. A two-dimensional electron gas (2DEG) in a magnetic field has electrons undergoing cyclotron orbits, quantized to Landau levels[6]. When a Landau level is filled, the Fermi energy is located between the Landau levels, separated by a gap $\hbar\omega_c$, where ω_c is the cyclotron frequency. Despite being somewhat analogous to a bulk insulator, the Hall conductance of the quantum Hall system is *perfectly quantized* to $\sigma_{xy} = n e^2/h$. The robust quantization, even in the presence of disorder, was explained by the existence of dissipationless states on the edge of the sample. These chiral edge states are protected from backscattering by a topological invariant known as Chern number, n[4].

B. The Quantum Spin Hall Effect

The requirement of an external magnetic field can be circumvented by including a spin-orbit coupling term, $\boldsymbol{L}\cdot\boldsymbol{S}$, which acts as an effective magnetic field, $\boldsymbol{B}_{\text{eff}}$. This was proposed in 1988 by Haldane for the honeycomb lattice[7], and later developed by Kane and Male as a prediction of the quantum spin Hall (QSH) effect[8–10].

Due to the chirality of spin-orbit coupling, the two edge states with opposite spins counterpropagate. This leads to a predicted quantized conductance $\sigma_{xx} = 2e^2/h$. The QSH effect was subsequently predicted and observed in HgTe quantum wells[11;12].

C. 3D Topological Insulators

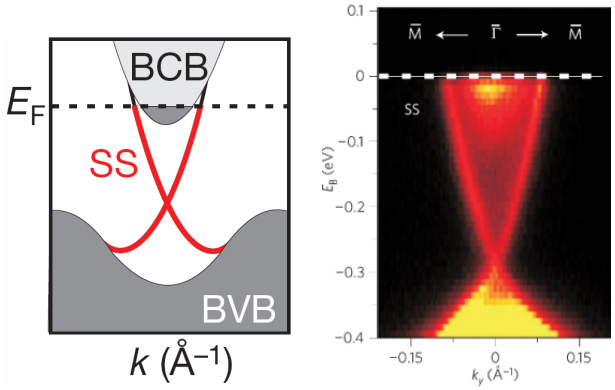

(a) Schematic of TI bands (b) ARPES on Bi_2Se_3

FIG. 1: Bandstructure of a prototypical single Dirac cone topological insulator. A schematic is shown in (a) with topologically protected surface states between bulk valence and conduction bands. The spin-polarized surface states can only intersect at Kramers points $(k = 0, \pi/a)$ due to time reversal symmetry. An ARPES measurement of the bandstructure of Bi_2Se_3 by Xia *et. al.* [13] is shown in (b).

As Hall conductivity measured in an external magnetic field is odd under time reversal, it is topologically distinct (topological class $\mathbb{Z}_2$) from the QSH state, where time reversal symmetry is unbroken[14]. There is a three-dimensional generalization of the QSH system with time reversal invariance (TRI). Physically, this corresponds to a 3D bulk insulator with counterpropagating spin-polarized surface states. There are four $\mathbb{Z}_2$ invariants $(\nu_0; \nu_1, \nu_2, \nu_3)$ associated with these 3D topological insulators[15] (TIs). $\nu_0 = 1$ defines a distinct phase called the strong topological insulator.

As the $\mathbb{Z}_2$ invariants require time reversal symmetry, the Hamiltonian for topological insulators is also required to be TRI. Kramers theorem requires that the eigenstates of such TRI Hamiltonians have a two-fold degeneracy, and thus so do the surface states. However for a crystal, there are certain TRI points in the Brillouin Zone (BZ), where these states $(\boldsymbol{k}_\uparrow, -\boldsymbol{k}_\downarrow)$ can cross, *viz.* $k = 0, \pm\pi/a$[15]. Thus the lowest order TRI Hamiltonian for the surface states is[14]

$$\mathcal{H}_{\text{surface}} = -i\hbar v_F\, \boldsymbol{\sigma} \cdot \boldsymbol{\nabla} \tag{1}$$

Here, v_F is the Fermi velocity and $\boldsymbol{\sigma}$ characterizes the fermion spin. Thus, the surface states have Dirac dispersion, with the Dirac cones centered at the Kramers points. Fu *et. al.* predicted Bi_xSb_{1-x} to be a 3D topological insulator[15], and this was experimentally verified by Hsieh *et. al.* using angle resolved photoemission spectroscopy (ARPES) with spin resolution[16;17]. In 2009, Bi_2Se_3 and Bi_2Te_3 were discovered to be single Dirac cone topological insulators[13;18–20], with the cone located at the BZ Center, Γ, as shown in Fig. 1. Due to their much simpler bandstructure and large bandgap, Bi_2Se_3 and Bi_2Te_3 have been the subject of much experimental and theoretical investigation since then.

II. A Warped Helical Fermi Surface

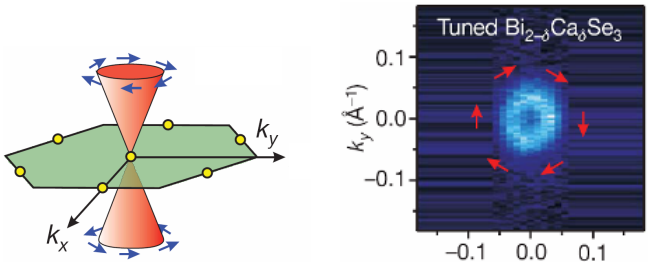

(a) Helical Dirac Cone in BZ (b) Fermi Surface of Bi_2Se_3

FIG. 2: Helicity and spin momentum locking in a single Dirac cone topological insulator, with schematic helical Dirac cone in (a) and a spin-resolved ARPES measurement of the Fermi surface of $Bi_{2-\delta}Ca_\delta Se_3$ in (b)[19]. The surface state momemtum, $k_{x,y}$ is locked to the spin $\sigma_{x,y}$ due to the $(\boldsymbol{k} \times \boldsymbol{\sigma})_z$ term in the surface state Hamiltonian.

Due to time reversal symmetry in a topological insulator, the surface states at a given energy form Kramers doublets $(\boldsymbol{k}_\uparrow, -\boldsymbol{k}_\downarrow)$. The Dirac cone is thus helical, and spin $\boldsymbol{\sigma}$ and momentum $\boldsymbol{k}$ are locked in the $x-y$ plane. For a mirror plane surface state, the Hamiltonian reads[14]

$$\mathcal{H}_{\text{surface}} \propto v_F\, (\boldsymbol{k} \times \boldsymbol{\sigma})_z \tag{2}$$

The spin-momentum locking for Bi_2Se_3 seen by spin-resolved ARPES[19] is shown in Fig. 2. As expected, the Fermi surface is isotropic and spin-polarized, in agreement with Eqn. 3. Notably, the helical arrangement of spins around the Dirac cone leads to a geometric Berry's phase of π. The spin polarization of the Fermi surface has been found to persist up to room temperature, suggesting possible spintronics applications[19].

A. Fermi Surface Warping in Bi_2Te_3

In contrast, ARPES studies of Bi_2Te_3 yielded slightly different results. Chen *et. al.*[20;21] found that at energies ε significantly above the Dirac point energy ε_D, the Fermi surface of Bi_2Te_3 is no longer circular. It becomes hexagonal at intermediate energies $(\varepsilon - \varepsilon_D)$ and hexagram, or

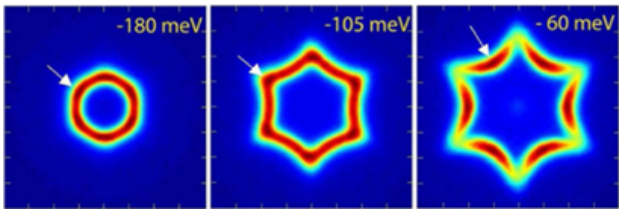

FIG. 3: ARPES studies of the evolution Fermi surface of Bi_2Te_3[21]. The Fermi surface evolves from an isotropic circle to a hexagon, and then to a hexagram (snow-flake shape) at increasing energies away from the Dirac point (-335 mV).

snow-flake like, at even higher energies, as shown in Fig. 3. The hexagonal deformation of the quasiparticle density of states was confirmed by scanning tunneling spectroscopy (STS) experiments[21;22].

The deformation of the Fermi surface was explained by Fu with addition of a warping term to the Hamiltonian[23] that introduces $x-y$ anistropy. The isotropic surface state Hamiltonian in Eqn. 3 can be written as

$$\mathcal{H}_0 \equiv v_F \left(k_x\sigma_y - k_y\sigma_x\right) \tag{3}$$

Noting that the Hamiltonian still has to obey the $\mathbb{C}_3$ crystal symmetry and TRI, the next order correction is not quadratic in k, but is instead cubic[23]

$$\begin{aligned}\mathcal{H}(\boldsymbol{k}) &= \varepsilon(\boldsymbol{k}) + v(\boldsymbol{k})\left(k_x\sigma_y - k_y\sigma_x\right) + \mathcal{H}_w \\ \mathcal{H}_w &= \frac{\lambda}{2}\left(k_+^3 + k_-^3\right)\sigma_z \end{aligned} \tag{4}$$

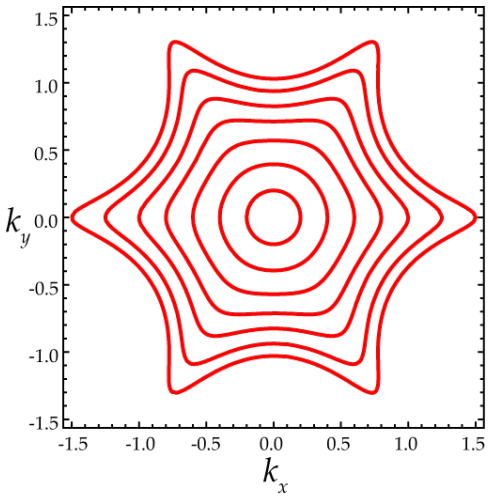

FIG. 4: A contour plot illustrating the evolution of the Fermi surface of Bi_2Te_3 using Eqn. 5, in units of $\sqrt{v/\lambda}$ using Mathematica©. Note that it reproduces the behavior in Fig. 3.

The $\varepsilon(\boldsymbol{k})$ term introduces particle-hole anisotropy and the second term corrects the Dirac velocity. The warping term, $\mathcal{H}_w$ has the underlying $\mathbb{C}_3$ crystal symmetry, is TRI, and introduces the anisotropy that we require. Using Eqn. 4, the surface state dispersion becomes

$$\varepsilon_\pm(\boldsymbol{k}) = \varepsilon_0(\boldsymbol{k}) \pm \sqrt{v(\boldsymbol{k})^2\boldsymbol{k}^2 + \lambda^2\boldsymbol{k}^6\cos^2(3\theta)} \tag{5}$$

Eqn. 5 contains the lowest order correction to the perfect helicity of the Dirac cone in Eqn. 3. The $\cos^2(3\theta)$ term is has six-fold symmetry, due to the $\mathbb{C}_3$ symmetry of the Hamiltonian and time reversal symmetry. Since $\mathcal{H}_w$ couples to σ_z, we expect some out-of-plane spin polarization at large enough $(\varepsilon - \varepsilon_D)$[1]. A contour plot of Eqn. 5 generated using Mathematica© is shown in Fig. 4. We see that it reproduces the behavior seen in ARPES experiments by Chen *et. al.*rather well. We note that spin-orbit coupling is expected to be stronger in Bi_2Te_3 than Bi_2Se_3, and thus the warping term $\mathcal{H}_w$ being observed in the former, but not the latter, is not surprising.

III. Spin Density Wave State in a Warped Dirac Cone

An isotropic Dirac cone as in the linear dispersion in Eqn. 3 in uninteresting from the perspective of competing order. However, the warping term $\mathcal{H}_W$ that introduces a hexagonal deformation in the Fermi surface, can lead to an instability in the Fermi surface. The helical nature of the Fermi surface leads us to consider the possibility of density waves with spin texture.

A. Nesting Conditions and Spin Density Waves

The one-dimensional electron gas has a Fermi surface consisting of two points separated by $2k_F$ in momentum space. The response of the 1D gas to perturbations of the Fermi surface, known as the Lindhard function[6;24], is

$$\chi(q) = -e^2\varrho\left(\varepsilon_F\right)\log\left|\frac{q+2k_F}{q-2k_F}\right| \tag{6}$$

Here $\varrho\left(\varepsilon_F\right)$ is the density of states at the Fermi energy ε_F. Thus the response function of a 1D gas diverges at wavevectors $q = 2k_F$, and external perturbations lead to a divergent charge redistribution. Thus at zero temperature, the gas is unstable to the formation of a periodically varying charge density or spin density[25;26], with the spatial periodicity λ_{DW} corresponding to $2k_F$

$$\lambda_{DW} = \frac{\pi}{k_F} \tag{7}$$

In higher dimensions, the number of states corresponding to *perfect Fermi surface nesting* ($q = 2k_F$) is

[1]The z-polarization $\langle\sigma_z\rangle$ has a periodicity of $\cos(3\theta)$ around the Fermi surface contour.

significantly reduced, and thus the singularity in $\chi(q)$ (Eqn. **??**) is removed. However, an anisotropic Fermi surface that does not disperse in certain directions results in parallel regions of the Fermi surface (i.e. large $\varrho(\varepsilon_F)$) separated by a nesting vector q_{DW}[25]. This leads to Fermi surface instabilities and a density wave in the q_{DW} direction.

Nesting across the Fermi surface with identical spins, *i.e.* $((k_1,\sigma),(k_2,\sigma))$, leads to a charge density wave (CDW) with no spin texture. In contrast, nesting with opposite spins, *i.e.* $((k_1,\sigma),(k_2,-\sigma))$ leads to a spin density wave (SDW) with no charge modulation. While a CDW state can be produced by electron-phonon coupling (Pierls distortion), a SDW requires significant electron-electron interactions (U). A textbook calculation finds the mean-field transition temperature to be[25]

$$k_B T_{SDW}^{MF} \sim \exp(-1/U\varrho(\varepsilon_F)) \tag{8}$$

B. Fermi Surface Nesting in Bi_2Te_3

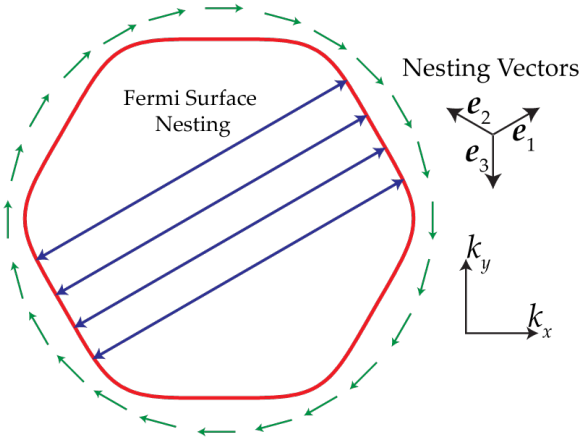

FIG. 5: A near-hexagonal Fermi surface contour of Bi_2Te_3 generated from Eqn. 5 for $\varepsilon = 0.7\sqrt{v/\lambda}$. The green arrows depict the $x-y$ spin polarization around the surface. Parallel regions of the Fermi surface support nesting in the directions labeled $e_{1,2,3}$.

In Fig. 3, we see that the Fermi surface of Bi_2Te_3 evolves from a circle to a hexagon, and then to a snowflake shape. In particular, for $0.55 < \varepsilon/\sqrt{v/\lambda} < 0.9$, the constant energy contours are nearly hexagonal[23]. As is clear in Fig. 5, there are three parallel regions of the Fermi surface, which support nesting, and thus the formation of density waves in the directions (e_1, e_2, e_3) with magnitude $2k_F$. We see in Fig. 5 that the surface state flips spin across the nesting vector, it cannot support a CDW. However this does allow us to consider the possibility of a SDW state below a critical temperature T_{SDW} for finite electron-electron interactions[23].

C. Landau–Ginzburg Theory of SDW State

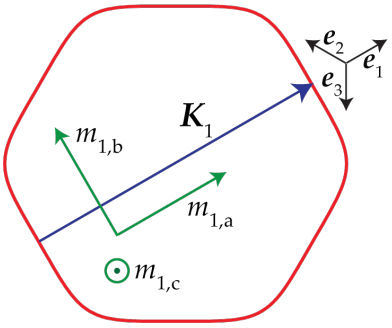

FIG. 6: The three-component order parameter of spin-texture for the nested hexagonal Fermi surface in Bi_2Te_3. The order parameter components are illustrated for the nesting vector $K_1 \parallel e_1$.

We start by defining the nesting vector as

$$K_i = 2k_F e_i, \quad i = 1,2,3 \tag{9}$$

The order parameters of a spin-texture phase (*e.g.* SDW) would relate to the magnetization in the three directions[2]. A density wave in momentum space corresponds to a particle-hole excitation $\hat{c}^\dagger_{k+K_i}\hat{c}_k$ along the nesting vector K_i. We use this to define the three-component order parameter $\vec{m}_i$. We pick the three components to be parallel and perpendicular to K_i, and along z respectively, as illustrated in Fig. 6. Thus we write the components of $\vec{m}_i$ as

$$\begin{aligned} m_{i,a} &= \sum_{\{k\}_{BZ}} \langle \hat{c}^\dagger_{k+K_i}\, e_i \cdot \sigma\, \hat{c}_k \rangle \\ m_{i,b} &= \sum_{\{k\}_{BZ}} \langle \hat{c}^\dagger_{k+K_i}\, (e_z \times e_i) \cdot \sigma\, \hat{c}_k \rangle \\ m_{i,c} &= \sum_{\{k\}_{BZ}} \langle \hat{c}^\dagger_{k+K_i}\, e_z \cdot \sigma\, \hat{c}_k \rangle \end{aligned} \tag{10}$$

To define the Landau–Ginzburg free energy, we first consider the symmetry operations that should leave the free energy $\mathcal{F}$ invariant. From §II., we note that $\mathcal{F}$ should be invariant under three-fold rotation C_3, time-reversal Θ, mirror reflection $\mathcal{M}$ and translation by an arbitrary vector r, $\mathcal{T}_r$. The components of the order parameter, $m_{i,\alpha}$ transform under these symmetry operations as follows

$$\begin{aligned} C_3 &: m_{i,\alpha} \to m_{i+1,\alpha} \\ \Theta &: m_{i,\alpha} \to -m_{i,\alpha} \\ \mathcal{M} &: m_{i,\alpha} \to m^*_{i+1,\alpha} \\ \mathcal{T}_r &: m_{i,\alpha} \to e^{iK_i\cdot r} m_{i,\alpha} \end{aligned} \tag{11}$$

[2] There is a finite spin-polarization in z due to $\mathcal{H}_W$ (Eqn. 4).

Due to TRI, $\mathcal{F}$ can only have even powers of $m_{i,\alpha}$, as can be seen from Eqn. 11. The lowest order term, apart from a constant, has to be quadratic in $m_{i,\alpha}$, *i.e.* of the form $m_{i,\alpha}\, m^*_{j,\beta}$, which now also accounts for mirror symmetry. The requirement of translational symmetry imposes an additional factor of δ_{ij}. Thus at quadratic order, the free energy can be written in terms of a susceptibility matrix, $\chi_{\alpha,\beta}$ as

$$\mathcal{F}_0 = \frac{1}{2}\,\chi_{\alpha,\beta} \sum_i m^*_{i,\alpha} m_{i,\beta} \tag{12}$$

The susceptibility matrix changes at a critical temperature T_c from a positive definite form to having a negative eigenvalue, and the ground state is in the SDW phase. The magnitude of the three order parameters $(m_{i,a}, m_{i,b}, m_{i,c})$ are significantly different. Since the Fermi surface is helical with spin polarization in the b direction, $m_{i,b}$ is likely to be the dominant term. The warping term $\mathcal{H}_W$ makes the $m_{i,c}$ term non-zero. in comparison, $m_{i,a}$ is likely to be very small. This would correspondingly affect the elements of the susceptibility matrix $\chi_{\alpha,\beta}$.

D. Cubic Anisotropy in SDW State

To quadratic order, the free energy $\mathcal{F}_0$ is symmetric in the order parameters $\{\vec{m}_i\}$. We can have an SDW state with the modulations in single or multiple directions being equally favorable in energy. This symmetry is broken by the quartic term in the free energy. For the rest of this section, we ignore the spin-polarization index α to concentrate on the directional anistropy (in $\{\boldsymbol{e}_i\}$) of the SDW. Thus, we write the quadratic term of the free energy as

$$\mathcal{F}_0 = t \sum_i \vec{m}_i^2 \tag{13}$$

We would expect the quartic term to be of the form $u\left(\sum_i \vec{m}_i^2\right)^2$. However, the cross terms $\vec{m}_i^2\, \vec{m}_j^2$ are excluded due to translational symmetry and thus we get the quartic correction

$$\mathcal{F}_1 = v \sum_i |\vec{m}_i|^4 \tag{14}$$

The quartic correction to the free energy ($\mathcal{F}_1$) breaks the SDW symmetry in the $x-y$ plane, and corresponds to *cubic anisotropy*[2]. For $v < 0$, the free energy is minimized by stripe order, *i.e.* the alignment of the SDW as a one-dimensional modulation along one of the nesting vectors $\boldsymbol{e}_i$. For $v > 0$, the energetically favorable order is diagonal, forming a two-dimensional lattice SDW with

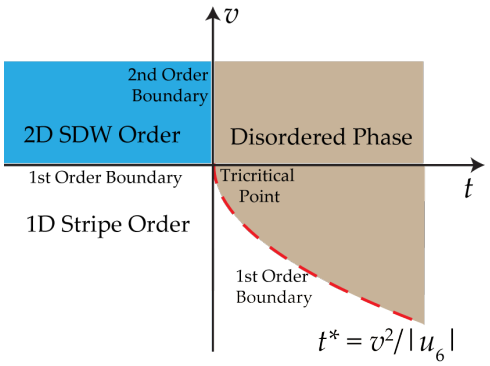

FIG. 7: The phase diagram in (t, u) parameter space of the anisotropic SDW instability of the Fermi surface.

$\{|\vec{m}_i|\}$ being all equal in the ordered phase. A sixth order term ensures stability in the phase diagram in the $v < 0$ region, given as

$$\mathcal{F}_2 = u_6 (m_1 m_2 m_3)^2 + u_6^* (m_1^* m_2^* m_3^*)^2 \tag{15}$$

Considering the free energy up to sixth order $\mathcal{F}^{(6)} = \mathcal{F}_0 + \mathcal{F}_1 + \mathcal{F}_2$ and using the saddle point approximation, we obtain the mean field phase diagram in the (t, v) plane shown in Fig. 7. The boundary between the 2D SDW phase and the disordered phase corresponds to a second order transition, whereas the boundary between the stripe phase both the other phases is a first order transition. We note the presence of a tricritical point in the phase diagram at $t = v = 0$.

IV. Conclusions and Related Work

We have elaborated on the work of Fu[23] that explained the evolution of the Fermi surface of Bi_2Te_3 as observed by ARPES using a warping term, $\mathcal{H}_{rmW}$ in the Hamiltonian. At intermediate energies $(\varepsilon - \varepsilon_D)$, the Fermi surface is hexagonal, and following Fu, we have explored the possibility of spin density wave order below a mean field temperature T_c. We have studied the free energy of the SDW phase in the Landau-Ginzburg framework and find a close correspondence to cubic anisotropy. Using this, we have constructed a phase diagram of spin order in on the hexagonal Fermi surface of Bi_2Te_3.

Looking to related topological insulators, the Fermi surface of Bi_xSb_{1-x} is much more complex. There are five surface states and a centrally deformed Dirac cone that displays hexagonal warping[16;17;27]. Due to the complexity of its bandsstructure, Bi_xSb_{1-x} still lacks a tractable theoretical model, but it still displays a π Berry's phase and weak anti-localization as observed in the 'simpler' TIs – Bi_2Se_3 and Bi_2Te_3[16;17]. It is likely that the nesting geometries would be more complex and also

more exotic in Bi_xSb_{1-x}.

There has also been some recent work in looking at topological phases in the honeycomb lattice in the strongly correlated limit[28;29]. Using the Hubbard model, the authors find that in the large U limit, the topological band insulator undergoes a phase transition to a SDW state, with order in the $x-y$ plane. There is an intermediate Mott Insulator phase which makes this system more exotic from the theoretical standpoint. The candidate topological Mott insulators, materials with strong correlations and strong spin-orbit coupling, are Ir-based pyrochlore oxides and organic materials, *e.g.* κ-$(BEDT\text{-}TTF)_2Cu_2(CN)_3$[29].

I acknowledge helpful advice and discussions with Dr. Liang Fu that were invaluable in the formulation and completion of this manuscript.

REFERENCES

[1] L D Landau and E.M. Lifshitz. *Statistical Physics, Part 1*. Butterworth-Heinemann, 3rd edition, 1980.

[2] Mehran Kardar. *Statistical Physics of Fields*. Cambridge University Press, 1st edition, June 2007.

[3] P.M. Chaikin and T.C. Lubensky. *Principles of Condensed Matter Physics*. Cambridge University Press, 1st edition, October 2000.

[4] J.E. Avron, Daniel Osadchy, and Ruedi Seiler. A topological look at the quantum Hall effect. *Physics Today*, 56(8):3842, August 2003.

[5] R.B. Laughlin. Quantized Hall conductivity in two dimensions. *Physical Review B*, 23(10):56325633, May 1981.

[6] Michael P. Marder. *Condensed Matter Physics*. Wiley-Interscience, 1st edition, 2000.

[7] F.D.M. Haldane. Model for a Quantum Hall Effect without Landau Levels: Condensed-Matter Realization of the "Parity Anomaly". *Physical Review Letters*, 61(18):2015–2018, October 1988.

[8] C.L. Kane and E.J. Mele. Quantum Spin Hall Effect in Graphene. *Physical Review Letters*, 95(22):226801, November 2005.

[9] C.L. Kane and E.J. Mele. $\mathbb{Z}_2$ Topological Order and the Quantum Spin Hall Effect. *Physical Review Letters*, 95(14):146802, September 2005.

[10] C.L. Kane. Graphene and the Quantum Spin Hall Effect. *International Journal of Modern Physics B*, 21(8 & 9):1155, 2007.

[11] B.A. Bernevig and Shou-Cheng Zhang. Quantum Spin Hall Effect. *Physical Review Letters*, 96(10):106802–4, March 2006.

[12] M. Koenig, Steffen Wiedmann, Christoph Brune, Andreas Roth, Hartmut Buhmann, L.W. Molenkamp, Xiao-Liang Qi, and Shou-Cheng Zhang. Quantum spin hall insulator state in HgTe quantum wells. *Science*, 318(5851):766, November 2007.

[13] Y. Xia, Dong Qian, David Hsieh, L.A. Wray, A. Pal, Hsin Lin, Arun Bansil, D. Grauer, Y.S. Hor, R.J. Cava, and M. Zahid Hasan. Observation of a large-gap topological-insulator class with a single Dirac cone on the surface. *Nature Physics*, 5(6):398–402, May 2009.

[14] M. Zahid Hasan and C.L. Kane. Topological Insulators. *arXiv:1002.3895*, February 2010.

[15] Liang Fu, C.L. Kane, and E.J. Mele. Topological Insulators in Three Dimensions. *Physical Review Letters*, 98(10):106803–4, March 2007.

[16] David Hsieh, Dong Qian, L.A. Wray, Y. Xia, Y.S. Hor, R.J. Cava, and M. Zahid Hasan. A topological Dirac insulator in a quantum spin Hall phase. *Nature*, 452(7190):970–4, April 2008.

[17] David Hsieh, Y. Xia, L.A. Wray, Dong Qian, A. Pal, J.H. Dil, J. Osterwalder, F. Meier, G. Bihlmayer, C.L. Kane, Y.S. Hor, R.J. Cava, and M. Zahid Hasan. Observation of unconventional quantum spin textures in topological insulators. *Science*, 323(5916):919–22, February 2009.

[18] H. Zhang, C.X. Liu, Xiao-Liang Qi, Xi Dai, Zhong Fang, and Shou-Cheng Zhang. Topological insulators in Bi_2Se_3, Bi_2Te_3 and Sb_2Te_3 with a single Dirac cone on the surface. *Nature Physics*, 5(6):438442, June 2009.

[19] David Hsieh, Y. Xia, Dong Qian, L.A. Wray, J.H. Dil, F. Meier, J. Osterwalder, L. Patthey, J.G. Checkelsky, N.P. Ong, A.V. Fedorov, H Lin, Arun Bansil, D. Grauer, Y.S. Hor, R.J. Cava, and M. Zahid Hasan. A tunable topological insulator in the spin helical Dirac transport regime. *Nature*, 460(7259):1101–5, August 2009.

[20] Y. L. Chen, James G. Analytis, J.-H. Chu, Z.K. Liu, S.-K. Mo, Xiao-Liang Qi, H J Zhang, D.H. Lu, Xi Dai, Zhong Fang, Shou-Cheng Zhang, Ian R. Fisher, Z Hussain, and Z.X. Shen. Experimental realization of a three-dimensional topological insulator, Bi_2Te_3. *Science*, 325(5937):178–81, July 2009.

[21] Zhanybek Alpichshev, James G. Analytis, J.-H. Chu, Ian R. Fisher, Y. L. Chen, Z.X. Shen, A. Fang, and A. Kapitulnik. STM Imaging of Electronic Waves on the Surface of Bi_2Te_3: Topologically Protected Surface States and Hexagonal Warping Effects. *Physical Review Letters*, 104(1):016401, January 2010.

[22] Tong Zhang, Peng Cheng, Xi Chen, Jin-Feng Jia, Xu-Cun Ma, Ke He, Li-Li Wang, Hai-Jun Zhang, Xi Dai, Zhong Fang, Xin-Cheng Xie, and Qi-Kun Xue. Experimental Demonstration of Topological Surface States Protected by Time-Reversal Symmetry. *Physical Review Letters*, 103(26):266803, December 2009.

[23] Liang Fu. Hexagonal Warping Effects in the Surface States of the Topological Insulator Bi_2Te_3. *Physical Review Letters*, 103(26):1–4, December 2009.

[24] Neil W. Ashcroft and N. David Mermin. *Solid State Physics*. Brooks Cole, 1st edition, 1976.

[25] George Grüner. *Density Waves in Solids*. Westview Press, 2000.

[26] G. Grüner. The dynamics of charge-density waves. *Reviews of Modern Physics*, 60(4):1129–1181, October 1988.

[27] Pedram Roushan, Jungpil Seo, C.V. Parker, Y.S. Hor, David Hsieh, Dong Qian, Anthony Richardella, M. Zahid Hasan, R.J. Cava, and Ali Yazdani. Topological surface states protected from backscattering by chiral spin texture. *Nature*, 460(7259):1106–1109, 2009.

[28] Stephan Rachel and Karyn Le Hur. Topological insulators and Spin-Charge separation from mott physics. *arXiv:1003.2238*, March 2010.

[29] Dmytro Pesin and Leon Balents. Mott physics and band topology in materials with strong spinorbit interaction. *Nature Physics*, 6(5):376–381, March 2010.